



Indoor/outdoor air exchange affects indoor radon – the use of a scale model room to develop a mitigation strategy

Carlo Lucchetti¹, Gianfranco Galli², and Paola Tuccimei³

¹Dipartimento di Scienze della Terra, “La Sapienza” Università di Roma, Roma, 00185, Italy

²Istituto di Geofisica e Vulcanologia, Roma, 00143, Italy

³Dipartimento di Scienze, Università “Roma Tre”, Roma, 00146, Italy

Correspondence: Paola Tuccimei (paola.tuccimei@uniroma3.it)

Received: 28 January 2022 – Revised: 20 April 2022 – Accepted: 31 May 2022 – Published: 15 June 2022

Abstract. Indoor/outdoor air exchange on indoor radon concentration was investigated. We evaluated the effect of air extraction versus air introduction at different flow rates on equilibrium ^{222}Rn activity concentrations in a scale model room of 62 cm × 50 cm × 35 cm (inner length × width × height), made of a porous, radium and thorium-rich lithoid ignimbrite (Tufo di Gallese) from Vico volcano (Lazio, central Italy). Experiments were carried either with the inner walls of the chamber covered with a plasterboard shield or without any inner coating. Air introduction was always more effective than air extraction to reduce indoor ^{222}Rn and, in both cases, higher flow rates produced higher ^{222}Rn decreases. The presence of the plasterboard enhanced ^{222}Rn reduction when outdoor air was introduced in the chamber. Main results were that, with plasterboard, maximum reductions of 89.5 % and 25.0 % were obtained introducing and extracting air, respectively; without plasterboard, we found maximum radon decreases of 33.2 % and 26.6 %, namely with air introduction or extraction. The diffusion of ^{222}Rn through the walls of the scale model room was modelled with a modified version of Fick’s second law, where a term considering air flow velocity was added. These findings suggested that the combined use of proper coatings on the inner walls of a house and outdoor air introduction at suitable rates are a good strategy to approach radon mitigation actions.

1 Introduction

Indoor radon accumulation is considered the main source of human exposition to ionizing radiation (NCRP, 2009; Radulescu et al., 2022). High levels of radon are generally due to the isotope ^{222}Rn , characterized by the longest half-life (about 3.8 d) and only occasionally the contribution of the isotope ^{220}Rn becomes significant: (i) in the basement of buildings rising over thorium-rich bedrocks; (ii) when thorium-rich building materials are used for construction. In these cases, ^{220}Rn with a very short half-life (56 s) may reach large activity concentrations.

Many studies dealt with experimental monitoring and mathematical modelling of indoor radon from soil and building materials in test houses (Capra et al., 1994; Font and Baixeras, 2003; Shaikh et al., 2003; Mancini et al., 2018) or modelled indoor radon concentration from experimental radon exhalation rates of building materials (Tuccimei et al., 2006; Kumar et al., 2014; Syuryavin et al., 2020).

The impact of environmental parameters on radon entry into buildings was addressed by many papers (Arvela et al., 2013; Vasilyev et al., 2015; Shen and Suuberg, 2016). Collignan and Powaga (2019) demonstrated that indoor environmental conditions (depressurization and air exchange rate) strongly affect radon entry and indoor radon activity concentrations. McGrath and Byrne (2018) experimentally validated model predictions for radon – ventilation relationships in retrofit buildings.

Tuccimei et al. (2009) proposed a classification of building materials based on the ^{222}Rn and ^{220}Rn exhalation rates required to attain predetermined indoor radon levels in a standard confined environment (the model room of 56 m³,

4 × 5 × 2.8 m, reported in EC, 1999) completely covered with the investigated material. The classification was to some extent modified years later (Cinelli et al., 2019). To our knowledge, no studies worked on a purpose-built scale model room to survey the contribution of building materials, radon proof membranes and air-exchange rate on indoor radon activity concentrations.

A scale model-room of 62 cm × 50 cm × 35 cm (inner length × width × height) was created with a very porous, ^{226}Ra -, ^{232}Th - and ^{40}K rich lithoid ignimbrite, called “Tufo di Gallese” to evaluate the contribution of building materials to indoor radon accumulation (Lucchetti et al., 2020). The model-room allows to study the effect of: (i) different types of covers (inner and outer) and (ii) air ventilation on indoor radon.

The outcomes of preliminary experiments (Lucchetti et al., 2020) indicate that equilibrium ^{222}Rn activities were reached rapidly (in just two days) when the chamber was left to exchange air through its walls consisting of a very porous rock (43 %). If the walls were externally coated with a transparent film used to conserve food, the air exchange was strongly reduced enhancing radon accumulation. Further tests demonstrated that inner covers (such as plasterboard and different kind of paints) partially reduced indoor ^{222}Rn , but entirely cut the short-lived ^{220}Rn . Finally, decreases of ambient temperature reduced radon exhalation from the building materials and, in turn, indoor activity concentration. In this paper, we present new experiments where indoor radon is monitored as a function of indoor/outdoor air exchange (air introduction versus air extraction at different flow rates), with or without inner plasterboard coating, to: (i) evaluate how the ventilation regime associated with the air permeability of a building affects indoor radon levels, and (ii) model the radon diffusion through the chamber walls.

2 Materials and methods

2.1 The scale model-room

As reported in Lucchetti et al. (2020), the model room was built with sixty blocks (15 cm × 10 cm × 5 cm per block) of “Tufo di Gallese” ignimbrite. Table 1 summarizes the main properties of this material. A cement mortar with very slight ^{222}Rn and ^{220}Rn exhalation rates was used to paste blocks. Only the walls of the room consisted of ignimbrite stone (surface area of 0.78 m²), whereas the floor and the roof were made from Plexiglas boards. The apparatus has been conceived to focus on the role of the walls made of a homogeneous radon-emitting building material on indoor radon concentration and considering its prevalent interaction with the outdoor environment. The inner volume of the chamber was about 0.110 m³. Two taps were applied on the upper Plexiglas board (Fig. 1) to connect the room with the input and

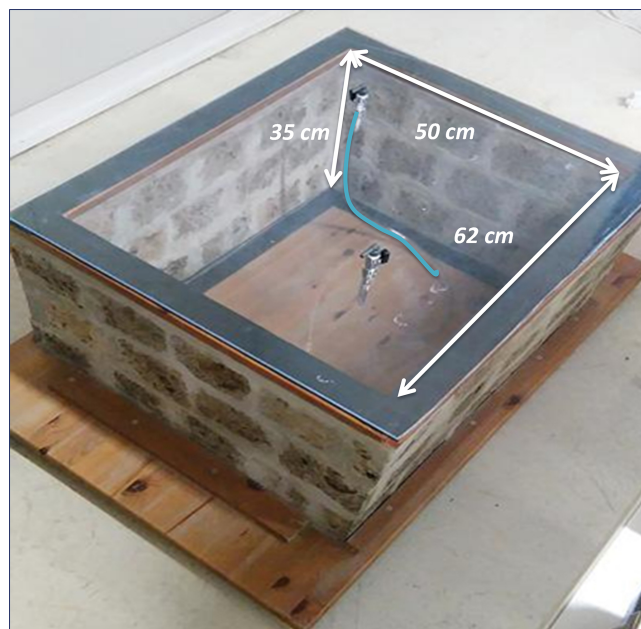


Figure 1. The scale model-room of 62 cm × 50 cm × 35 cm (inner length × width × height), made of “Tufo di Gallese” ignimbrite (Caprarola area, central Italy). Two taps are installed on the Plexiglas roof of the room to introduce and/or extract air from the chamber.

output openings of the RAD7 monitor via the vinyl tubing provided by DurrIDGE Company Inc.

2.2 Indoor radon determination

Two kinds of experiments were accomplished: (1) introduction of outdoor air in the model room; (2) extraction of indoor air from the model room. The tests were repeated either with internal coatings on the chamber walls or without them. Just ^{222}Rn , hereafter called radon, was considered.

In the first type of experiments, indoor radon activity concentration was measured using the AER PLUS (Algae Instrumentation) radon monitor. It is a small sized commercial solid-state radon detector, with local storage for temperature and relative humidity data. It is battery supplied with an autonomy of one year. The instrument was calibrated at Istituto Nazionale di Geofisica e Vulcanologia (INGV, Roma, Italy) and compared with other instruments such as RAD7. The effect of water molecules on AER PLUS efficiency was evaluated (Galli et al., 2019).

In the second type of experiments, indoor radon activities concentration was measured using either AER PLUS (Algae Instrumentation) or RAD 7 (DurrIDGE co.). RAD 7 is an electrostatic chamber equipped with a solid-state silicon detector, operated at a nominal voltage of 2000–2500 V for the collection of radon daughters onto its surface. The sensor detects and separates alpha particles on their energy basis. This allows to select only the short-lived ^{218}Po (with a half-life of

Table 1. Porosity, ^{232}Th , ^{226}Ra and ^{40}K specific activities and ^{222}Rn and ^{220}Rn exhalation rates of “Tufo di Gallese” ignimbrite.

Material	Porosity %	^{232}Th Bq kg^{-1}	^{226}Ra Bq kg^{-1}	^{40}K Bq kg^{-1}	E_{222} $\text{Bq m}^{-2} \text{h}^{-1}$	E_{220} $\text{Bq m}^{-2} \text{h}^{-1}$
Tufo di Gallese	43	290 ± 5	190 ± 3	2239 ± 28	5.91 ± 0.14	6434 ± 494

about 3 min) to measure ^{222}Rn , reaching the radioactive equilibrium between them in just 15 min. This option (the Sniff mode, according to RAD7 protocols) allows to change experimental conditions fast and perform rapidly the test. Temperature and relative humidity are recorded inside the instrument and a pump guarantees the air circulation in the set-up. A cylinder of desiccant (drierite) was placed before the inlet of RAD7 to reduce air humidity. Indoor air was sampled from the model room and then transferred to the radon monitor. ^{222}Rn activity concentration was corrected for effect of water molecules on the electrostatic collection of ^{218}Po ions onto the surface of the silicon detector (neutralization) according to De Simone et al. (2016).

2.2.1 Experiments with the inner coating

As anticipated in Sect. 2.2, two types of experiments were carried out to evaluate the relative change of indoor radon in the model room under different experimental conditions. Firstly, the model room was internally covered with a shield of plasterboard with a double coat of paint to simulate the walls of a building where the bricks are covered with plaster and paint.

Starting from a reference equilibrium radon level ($Rn_{\text{no ventilation}}$) reached with the two taps on the chamber roof closed (see Fig. 1), air exchange between the room and the outer environment was appropriately induced and controlled. The average ^{222}Rn level in the laboratory was 30 Bq m^{-3} , with no detectable ^{220}Rn . Then, outer air was introduced, or indoor air extracted from the model room at different flow rates and indoor radon concentration was monitored up to new equilibrium concentration ($Rn_{\text{air ventilation}}$). Relative change of Indoor Radon (RIR) was expressed following Eq. (1):

$$\text{RIR} = \frac{Rn_{\text{air ventilation}} - Rn_{\text{no ventilation}}}{Rn_{\text{no ventilation}}} \times 100 \quad (1)$$

The value is negative in case of radon reduction, positive for radon increase.

In the first set of tests, we evaluated the effect of outer air introduction in the model room through a tap and with the other closed, to simulate the effect of the room overpressure on indoor radon levels. The pump of RAD7 was employed to drive air in with variable air flow rates (AFR): 0.82, 0.64, 0.50, 0.30 and 0.15 L min^{-1} . These conditions were obtained and controlled using two flowmeters appropriately coupled to a T-joint, with one flowmeter connected to RAD7 and used

to check the air flow and the other just employed to reduce the air flow. Indoor radon was measured with the AER PLUS placed in the model room, with RAD7 acting just as a pump.

In the second group of experiments, indoor air was extracted from the model room through a tap, with a flow rate of 0.82, 0.50 and 0.15 L min^{-1} . The experimental set-up was like that of the first set of trials, with the second tap closed and RAD7 used to monitor indoor radon levels. The goal of these experiments was to evaluate the influence of enhanced indoor depression on radon activity concentrations. In order to make the results of the experiments more exportable, the air flow rates (L min^{-1}) were expressed as air exchange rates (ACH, h^{-1}) by dividing air flow rates (AFR) by the volume of the model room (V) and multiplying by 60.

$$\text{ACH} = \frac{\text{AFR}}{V} \times 60 \quad (2)$$

2.2.2 Experiments without the inner coating

Finally, the plasterboard shield was removed from the inner walls of the room; outdoor air was introduced, and indoor air was extracted from the chamber at 0.50 and 0.82 L min^{-1} . In both cases, indoor radon was compared with the equilibrium value reached without ventilation. Outdoor radon concentration in contact with the room walls, at 5 and 10 cm distance was monitored. The results of these tests were modelled with the Fick's second law.

2.3 Modelling radon diffusion through the room walls

In order to model radon diffusion through the room walls (Sasaki et al., 2007; Savović and Djordjević, 2008; Savović et al., 2011; Urošević and Nikezić, 2008), we applied a modified version of Fick's second law, where we added a term (second term of Eq. 3) to consider the air flow velocity, thus modelling a diffusive-advective transport (Chakraverty et al., 2018):

$$\frac{dC(x,t)}{dt} = D \frac{d^2C(x,t)}{dx^2} - v \frac{dC(x,t)}{dx} + g - \lambda C(x,t) \quad (3)$$

where: $C(x,t)$ is the radon concentration in the pore space of the building material (Bq m^{-3}) that depends on location x and time t , D is the radon diffusion coefficient ($\text{m}^2 \text{ s}^{-1}$), x is the distance from the inner side of the wall to the outdoor direction (m), v is the air velocity through the wall (m s^{-1}), g is the radon creation rate per unit size of the pores ($\text{Bq m}^{-3} \text{ s}^{-1}$), and λ is the radon decay constant (s^{-1}).

3 Results

Results of all experiments are reported in Table 2.

An example of indoor radon monitoring during the experiments and data treatment is provided by experiment 1 (Fig. 2), where radon activity concentration was measured in the model room using the AER PLUS instrument. In the first four days, ^{222}Rn was recorded in the room with the two taps closed. After two days, equilibrium level ($\text{Rn}_{\text{no ventilation}}$) was almost reached (about 641 Bq m^{-3}) and at the end of the fourth day, outdoor air was introduced in the room with a flow rate of 0.82 L min^{-1} . After ten hours new equilibrium ^{222}Rn concentration was attained (about 67 Bq m^{-3}) and RIR was calculated (-89.5% , see Table 2). The same approach was applied to all tests.

The first group of experiments clearly shows that the introduction of outdoor air in the model room, internally covered with a layer of plasterboard, strongly reduces indoor radon concentration from -63.8% with air flow of 0.15 L min^{-1} to -89.5% with flow of 0.82 L min^{-1} (Table 2), demonstrating that RIR is directly proportional to the air flow. On the other hand (second group of experiments), the extraction of indoor air from the room with the plasterboard coating moderately cuts radon level from -4.7% with air flow of 0.15 L min^{-1} to -25% with flow of 0.82 L min^{-1} (Table 2).

Finally, we removed the plasterboard from the inner side of the model room and performed four further experiments (experiments from 9 to 12, see Table 2). In this experimental condition (third group of experiments), RIR values were extremely reduced in the “introduction of air” experiments compared with corresponding tests with the plasterboard coating (group 1, Fig. 3). For example, experiment 1 provided RIR of -89.5% with air flow of 0.82 L min^{-1} and experiment 6, RIR of -33.2 with the same flow. A direct correlation of RIR and air flows is also confirmed in tests of group 3. Experiments of group 4 (“extraction of air” type, without the plasterboard) provided results that correspond within the error range to those of group 2 experiments (Table 2 and Fig. 3), suggesting that the presence of the plasterboard does not improve the effectiveness of the air exchange like in the “introduction of air” experiments.

4 Discussion

4.1 The influence of indoor/outdoor air-exchange on radon levels with the inner coating on the room walls

These experiments allowed us to simulate the effect of indoor/outdoor air-exchange on indoor radon levels. The scale model-room simulates the effect of building materials with high radon exhalation rates on indoor radon activity concentration. The high porosity of “Tufo di Gallese” ignimbrite,

when the chamber is not coated with inner covers, enhances the effect of natural ventilation on indoor radon levels.

A common practice to reduce indoor radon makes use of air fans which extract indoor air from the room. If air exchange rates (ACH) are low and radon concentrations are very high, radon-rich air is more effectively pumped in, producing a modest effect on radon concentration (see results of second groups of experiments).

According to the experiments, a better result is reached if radon-free outdoor air is injected into the room, producing an overpressure that strongly reduced the entry of radon-rich air from the building materials (see first group of experiments), a porous ignimbrite with high ^{222}Rn and ^{220}Rn exhalation rates (see Table 1).

The presented tests show that indoor radon is strongly affected by air ventilation and that the higher the flow rates the stronger the radon decrease. This finding agrees with measurements carried out by Syuryavin et al. (2020) that investigated the effect of air exchange on indoor radon and thoron from a low dense building materials placed in a perfectly sealed chamber. They obtained ^{222}Rn decreases up to 66 times from experiments with ACH of 0.50 h^{-1} compared with correspondent no air exchange measurements. This reduction is much higher than those obtained exchanging air at the same rate from the presented model room, because “Tufo di Gallese” ignimbrite is very porous, even if internally covered with the plasterboard (Table 2).

4.2 The influence of indoor/outdoor air-exchange on radon levels without the inner coating on the room walls

Experiments of groups 3 and 4 carried out without the plasterboard on the inner walls of the room lowered the ability of air ventilation to reduce indoor radon concentration. In the “introduction of air” tests (group 3) the decreased efficiency of air exchange compared with that of the experiments of group 1 (with the plasterboard) is due to the enhanced air exchange through the very porous building material that reduce the overpressure and the radon discharge outwards. Also in this case, the limited reduction of indoor radon is directly correlated with air flow (Fig. 3).

The comparison between the “extraction of air” experiments accomplished with the plasterboard (group 2) and without it (group 4) show no significant differences in the results because the air exchange is not strong enough to produce a large underpressure and remove indoor radon. On the contrary, the porosity of the “Tufo di Gallese” seems to favour, even if only slightly, the radon release outward in the experiments without the plasterboard.

This physical behaviour was modelled applying the Fick’s second Law (see Eq. 3) to experiments of groups 3 and 4. The graphical solutions of the modelling are reported in Fig. 4a (air introduction) and 4b (air extraction). Table 3 reports the values of parameters used for modelling.

Table 2. Relative change of Indoor Radon (RIR) in the model room with and without the plasterboard inner covers in a series of experiments where outdoor air was introduced in the model room or indoor air was extracted from the model room at different air flow and air exchange (ACH) rates.

Experiment	Air flow (L min ⁻¹)	Air Exchange Rate (h ⁻¹)	Relative change of Rindoor radon
Group 1, with inner cover		Air in	
1	0.82	0.49	-89.5 (±4.2)
2	0.64	0.38	-88.8 (±4.3)
3	0.5	0.30	-82.7 (±3.5)
4	0.3	0.18	-75.6 (±4.4)
5	0.15	0.09	-63.8 (±4.8)
Group 2, with inner cover		Air out	
6	-0.82	-0.49	- 25.0 (±5.7)
7	-0.5	-0.30	- 22.4 (±2.5)
8	-0.15	-0.09	- 4.7 (±4.7)
Group 3, no inner cover		Air in	
9	0.82	0.49	-33.2 (±3.8)
10	0.5	0.30	-26.4 (±2.3)
Group 4, no inner cover		Air out	
11	-0.82	-0.49	-26.6 (±3.7)
12	-0.5	-0.30	-24.8 (±2.7)

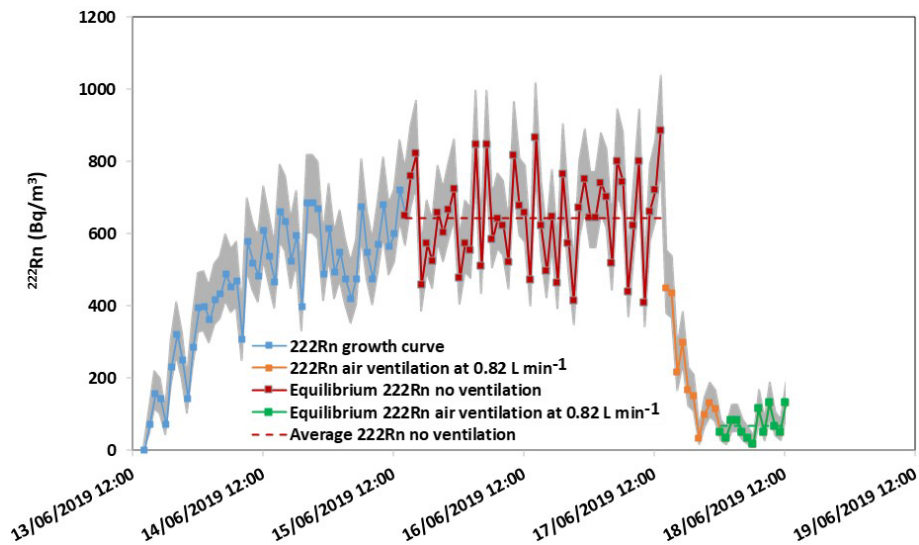


Figure 2. ²²²Rn activity concentration versus time during experiment 1 (first group of experiments). Radon data were recorded hourly. The relative standard deviation is about 40 % at 100 Bq m⁻³, about 18 % at 500 Bq m⁻³ and about 13 % at 1000 Bq m⁻³. The grey band shows data uncertainties (one standard deviation).

Figure 4a shows a first curve of radon diffusion through the room walls, labelled “0 L min⁻¹, year 2020”, where the real measurements of laboratory background at increasing distances from the chamber walls were not taken into consideration, but an average value of 30 Bq m⁻³ was hypothesised. The shape of this curve does not reproduce the real

shift of radon from the room walls outward. On the other end, the other curves at air flow rates of 0, 0.5 and 0.82 L min⁻¹ rely on the experimental measurements of radon levels at increasing distance from the walls. These outdoor data are much higher than 30 Bq m⁻³ and display a decreasing trend moving away from the wall. The diffusion curves trough the

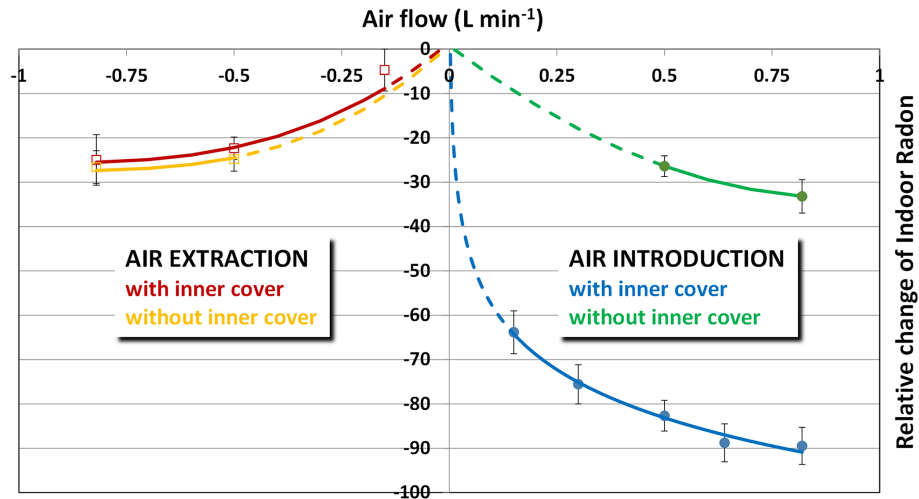


Figure 3. Relative change of Indoor ^{222}Rn (RIR) at different air flows with or without a plasterboard coating the inner walls of the model room. RIR is equal to $(R_{n\text{air ventilation}} - R_{n\text{no ventilation}})/(R_{n\text{no ventilation}}) \times 100$. Green and blue curves on the right stand for RIR obtained in the “introduction of air” experiments of groups 1 (from test 1 to 5) and 3 (experiments 9 and 10); red and orange curves on the left side of the plot correspond to RIR recorded in the “extraction of air” experiments of groups 2 (from test 6 to 8) and 4 (experiments 11 and 12).

Table 3. Parameters used in the modelling using the Fick’s second law (Eq. 3).

Parameter	Label	Value	Unity
Radon diffusion coefficient ^a	D	2.54×10^{-6}	$\text{m}^2 \text{s}^{-1}$
Radon emanation factor ^b	η	0.65	adimensional
Density ^c	ρ	2310	kg m^{-3}
^{226}Ra specific activity ^c	a	190	Bq kg^{-1}
^{222}Rn decay constant	λ	2.09794×10^{-6}	s^{-1}
Porosity ^c	p	0.43	adimensional

^a Narula et al. (2010), datum referred to a porous material with a density like that of “Tufo di Gallese” ignimbrite. ^b Righi et al. (2006). ^c Lucchetti et al. (2020).

building material are characterised by a first part with increasing values and then by a decreasing trend. These results demonstrate very well the outward forced flow of radon, induced by the air introduction.

Figure 4b reports the modelling of experiments of group 4. The shape of the curves is much different from that of group 3 tests (Fig. 4a) since external air is drawn through a very porous material into the chamber. As a result, the outdoor air is enriched in radon along its way to the room.

5 Conclusions

These experiments demonstrate that the application of air exchange and the contemporaneous use of coatings applied on the inner walls of a buildings made of radon-rich materials enhance indoor radon reduction. Outdoor air introduction increases the indoor pressure of the room, reducing radon entry and pushing radon outwards. If the outer walls are not sealed by cement or mortar, radon diffusion out of the building is even more facilitated.

Conversely, the extraction of indoor air is less effective than air introduction, regardless of the plasterboard cover, because the room pressure is slightly decreased, and radon exhaled from the building material more easily enters the room.

This suggests the use of a combined mitigation strategy to cut indoor radon levels, consisting of effective air exchange and the application of suitable radon-proof membrane on the inner walls of a room to prevent radon entry from the room walls. It is also recommended to avoid unnecessary coatings on the external wall surfaces, to make the reduction of indoor radon more effective when a room overpressure is applied. Findings of this work directly apply to radium-rich building materials and to the use of air exchange. Mixed mitigation strategies should consider the specific radium content of building materials and guarantee: (i) a low degree of noise since ventilation should not be so annoying, (ii) comfortable indoor temperature and humidity conditions either in winter or summer, and (iii) a sustainable energy consumption.

Future studies will focus on the determination of radon diffusion coefficients of commercial and new radon-proof ma-

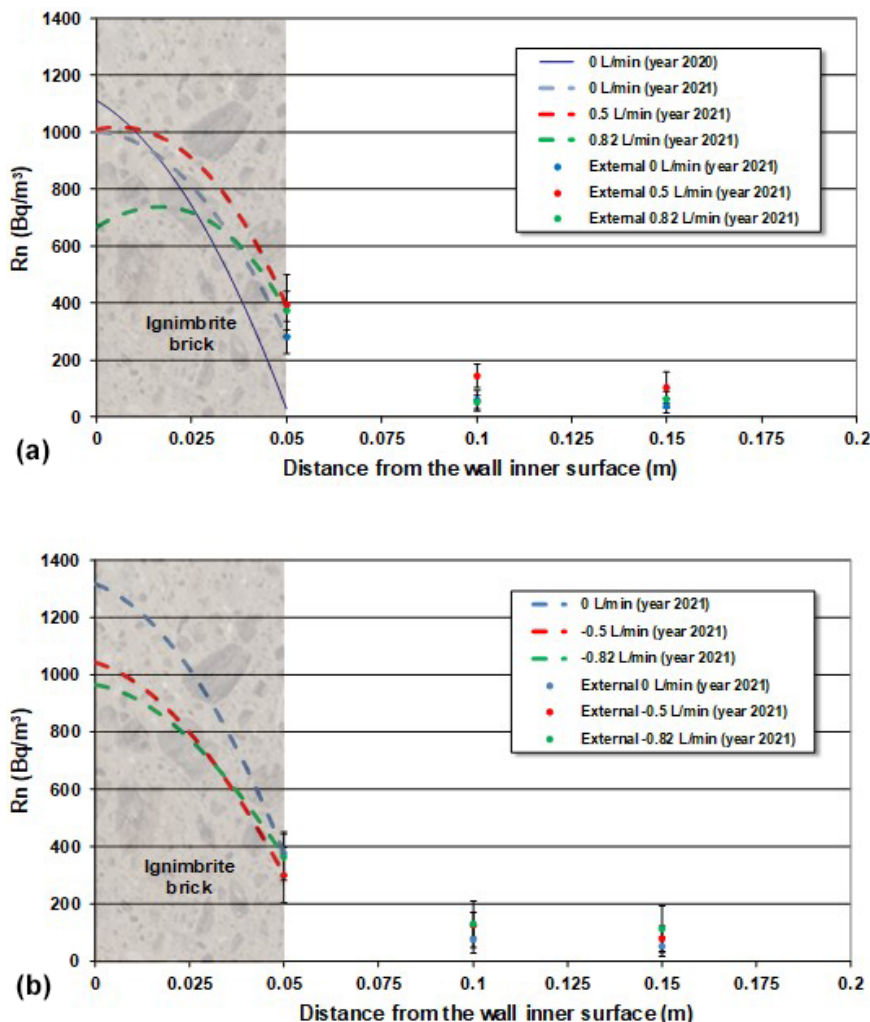


Figure 4. Radon diffusion through the wall of the scale model room according to Eq. (3). **(a)** Introduction of outdoor air in the model room at 0.5 and 0.82 L min⁻¹, compared with the no ventilation experiment. The curve at 0 L min⁻¹ of year 2020 does not take into consideration the real measurements of laboratory background at increasing distances from the chamber walls, but just an average value of 30 Bq m⁻³. **(b)** Extraction of indoor air from the model room at 0.5 and 0.82 L min⁻¹, compared with the no ventilation experiment.

terials that will be then applied on the presented model room where proper air exchange will be reconstructed.

Code and data availability. All data and equations are reported in the manuscript. Equations are in Sect. 2, data in Sects. 3 and 4. The reader is referred to Table 2, Figs. 2, 3 and 4 for data presentation.

Author contributions. CL, GG and PT designed the experiments and carried them out. GG and PT developed the model code and performed the simulations. GG and PT prepared the manuscript with contributions from CL.

Competing interests. The contact author has declared that neither they nor their co-authors have any competing interests.

Disclaimer. Publisher's note: Copernicus Publications remains neutral with regard to jurisdictional claims in published maps and institutional affiliations.

Special issue statement. This article is part of the special issue "Geoscience applications of environmental radioactivity (EGU21 GI6.2 session)". It is a result of the EGU General Assembly 2021, 19–30 April 2021.

Review statement. This paper was edited by Gerti Xhixha and reviewed by two anonymous referees.

References

- Arvela, H., Holmgren, O., Reisbacka, H., and Vinha, J.: Review of low-energy construction, air tightness, ventilation strategies and indoor radon: results from Finnish houses and apartments, *Radiat. Prot. Dosim.*, 162, 51–63, <https://doi.org/10.1093/rpd/nct278>, 2013.
- Capra, D., Silibello, C., and Queirazza, G.: Influence of Ventilation Rate on Indoor Radon Concentration in a Test Chamber, *Radiat. Prot. Dosim.*, 56, 15–18, <https://doi.org/10.1093/oxfordjournals.rpd.a082414>, 1994.
- Chakraverty, S., Sahoob, B. K., Rao, T. D., Karunakara, P., and Saprab, B. K.: Modelling uncertainties in the diffusion-advection equation for radon transport in soil using interval arithmetic, *J. Environ. Radioactiv.*, 182, 165–171, <https://doi.org/10.1016/j.jenvrad.2017.12.007>, 2018.
- Cinelli, G., De Cort, M., and Tollefsen, T. (Eds.): European Atlas of Natural Radiation, Publication Office of the European Union, Luxembourg, 195 pp., nline version <https://doi.org/10.2760/46388>, 2019.
- Collignan, B. and Powaga, E.: Impact of ventilation systems and energy savings in a building on the mechanisms governing the indoor radon activity concentration, *J. Environ. Radioactiv.*, 196, 268–273, <https://doi.org/10.1016/j.jenvrad.2017.11.023>, 2019.
- De Simone, G., Lucchetti, C., Galli, G., and Tuccimei, P.: Correcting for H₂O interference using electrostatic collection-based silicon detectors, *J. Environ. Radioactiv.*, 162–163, 146–153, <https://doi.org/10.1016/j.jenvrad.2016.05.021>, 2016.
- EC (European Council), Directorate-General for Environment: Radiological protection principles concerning the natural radioactivity of building material, *Radiation Protection* 112, 16 pp., 1999.
- Font, L. and Baixeras, C.: The RAGENA dynamic model of radon generation, entry and accumulation indoors, *Sci. Total Environ.*, 307, 55–69, [https://doi.org/10.1016/S0048-9697\(02\)00462-X](https://doi.org/10.1016/S0048-9697(02)00462-X)2003, 2003.
- Galli, G., Cannelli, V., Nardi, A., and Piersanti, A.: Implementing soil radon detectors for long term continuous monitoring, *Appl. Radiat. Isotopes*, 153, 108813, <https://doi.org/10.1016/j.apradiso.2019.108813>, 2019.
- Kumar, A., Chauhan, R. P., Joshib, M., and Sahoo, B. K.: Modeling of indoor radon concentration from radon exhalation rates of building materials and validation through measurements, *J. Environ. Radioactiv.*, 127, 50–55, <https://doi.org/10.1016/j.jenvrad.2013.10.004>, 2014.
- Lucchetti, C., Castelluccio, M., Altamore, M., Galli, G., Soligo, M., Tuccimei, P., and Voltaggio, M.: Using a scale model room to assess the contribution of building material of volcanic origin to indoor radon, *Nukleonika*, 65, 71–76, <https://doi.org/10.2478/nuka-2020-0010>, 2020.
- Mancini, S., Guida, M., Cuomo, A., Guida, D., and Ismail, A. H.: Modelling of indoor Radon activity concentration dynamics and its validation through in-situ measurements on regional scale, *AIP Conf. Proc.*, 1982, 020043, <https://doi.org/10.1063/1.5045449>, 2018.
- McGrath, J. A. and Byrne, M. A.: The Relationship between Radon and Ventilation in Retrofit Buildings: Experimental Validation of Model Predictions, Sustainable Energy Authority of Ireland (SEAI), RRD/00128, 22 pp., 2018.
- Narula, A. K., Chauhan, R. P., and Chakarvati, S. K.: Testing permeability of building materials for radon diffusion, *Indian Journal of Pure and Applied Physics*, 48, 505–507, 2010.
- NCRP (National Council on Radiation Protection and Measurements): Ionizing Radiation Exposure of the Population of the United States, Report n. 160, ISBN-13: 978-0-929600-98-7, 2009.
- Radulescu, I., Calin, M. R., Luca, A., Röttger, A., Grossi, C., Done, L., and Ioan, M. R: Inter-comparison of commercial continuous radon monitors responses, *Nucl. Inst. Meth Phys. Res. A*, 1021, 165927, <https://doi.org/10.1016/j.nima.2021.165927>, 2022.
- Righi, S., Coatti F., Bargossi, G. M., Verità, S., and Bruzzi, L.: Emanazione di radon da materiali lapidei naturali. Atti del Terzo Convegno Nazionale Controllo ambientale degli agenti fisici: dal monitoraggio alle azioni di risanamento e bonifica, Biella 7–9 giugno 2006, Gamma Servizi, ISBN 8874790333, 2006.
- Sasaki, T., Gunji, Y., and Iida, T.: Transient-Diffusion Measurements of Radon: Practical Interpretation of Measured Data, *J. Nucl. Sci. Technol.*, 44, 1032–1037, <https://doi.org/10.1080/18811248.2007.9711343>, 2007.
- Savović, S. and Djordjevich, A.: Numerical solution of the diffusion equation describing the flow of radon through concrete, *Appl. Radiat. Isotopes*, 66, 552–555, <https://doi.org/10.1016/j.apradiso.2007.08.018>, 2008.
- Savović, S., Djordjevich, A., Tse, P. W., and Nikezic, D.: Explicit finite difference solution of the diffusion equation describing the flow of radon through soil, *Appl. Radiat. Isotopes*, 69, 237–240, <https://doi.org/10.1016/j.apradiso.2010.09.007>, 2011.
- Shaikh, A. N., Ramachandran, T. V., and Vinod Kumar, A.: Monitoring and modelling of indoor radon concentrations in a multi-storey building at Mumbai, India, *J. Environ. Radioactiv.*, 67, 15–26, [https://doi.org/10.1016/S0265-931X\(02\)00144-3](https://doi.org/10.1016/S0265-931X(02)00144-3), 2003.
- Shen, R. and Suuberg, E. M.: Impacts of changes of indoor air pressure and air exchange rate in vapor intrusion scenarios, *Build. Environ.*, 96, 178–187, <https://doi.org/10.1016/j.buildenv.2015.11.015>, 2016.
- Suryavin, A. C., Park, S., Nirwono, M. M., and Lee, S. H.: Indoor radon and thoron from building materials: Analysis of humidity, air exchange rate, and dose assessment, *Nucl. Eng. Technol.*, 52, 2370–2378, <https://doi.org/10.1016/j.net.2020.03.013>, 2020.
- Tuccimei, P., Moroni, M., and Norcia, D.: Simultaneous determination of ²²²Rn and ²²⁰Rn exhalation rates from building materials used in Central Italy with accumulation chambers and a continuous solid state alpha detector: influence of particle size, humidity and precursors concentration, *Appl. Radiat. Isotopes*, 64, 254–263, <https://doi.org/10.1016/j.apradiso.2005.07.016>, 2006.
- Urošević, V. and Nikezić, D.: Simulation diffusive and advective transport of radon gas through concrete samples, 12th International Research/Expert Conference “Trends in the Development of Machinery and Associated Technology”, TMT 2008, Istanbul, Turkey, <https://doi.org/10.1093/rpd/ncn077>, 26–30 August 2008.
- Vasilyev, A. V., Yarmoshenko, I. V., and Zhukovsky, M. V.: Low air exchange rate causes high indoor radon activity concentration in energy-efficient buildings, *Radiat. Prot. Dosim.*, 164, 601–605, <https://doi.org/10.1093/rpd/ncv319>, 2015.